JOURNAL OF VIROLOGY, Feb. 2011, p. 1793–1803 Vol. 85, No. 4
0022-538X/11/$12.00 doi:10.1128/JVI.01924-10


# Impact of Valency of a Glycoprotein B-Specific Monoclonal Antibody on Neutralization of Herpes Simplex Virus▽

Adalbert Krawczyk,[1]§ Jürgen Krauss,[1] Anna M. Eis-Hübinger,[2] Martin P. Däumer,[2]† Robert Schwarzenbacher,[3] Ulf Dittmer,[4] Karl E. Schneweis,[3] Dirk Jäger,[1] Michael Roggendorf,[4] and Michaela A. E. Arndt[1]*

*National Center for Tumor Diseases, University of Heidelberg, 69120 Heidelberg, Germany[1]; Institute of Virology, University Medical Center Bonn, 53105 Bonn, Germany[2]; Department of Molecular Biology, University of Salzburg, Salzburg, Austria[3]; and Institute of Virology, University Hospital Essen, University of Duisburg-Essen, 45147 Essen, Germany[4]*

Received 10 September 2010/Accepted 18 November 2010

**Herpes simplex virus (HSV) glycoprotein B (gB) is an integral part of the multicomponent fusion system required for virus entry and cell-cell fusion. Here we investigated the mechanism of viral neutralization by the monoclonal antibody (MAb) 2c, which specifically recognizes the gB of HSV type 1 (HSV-1) and HSV-2. Binding of MAb 2c to a type-common discontinuous epitope of gB resulted in highly efficient neutralization of HSV at the postbinding/prefusion stage and completely abrogated the viral cell-to-cell spread *in vitro*. Mapping of the antigenic site recognized by MAb 2c to the recently solved crystal structure of the HSV-1 gB ectodomain revealed that its discontinuous epitope is only partially accessible within the observed multidomain trimer conformation of gB, likely representing its postfusion conformation. To investigate how MAb 2c may interact with gB during membrane fusion, we characterized the properties of monovalent (Fab and scFv) and bivalent [IgG and F(ab′)$_2$] derivatives of MAb 2c. Our data show that the neutralization capacity of MAb 2c is dependent on cross-linkage of gB trimers. As a result, only bivalent derivatives of MAb 2c exhibited high neutralizing activity *in vitro*. Notably, bivalent MAb 2c not only was capable of preventing mucocutaneous disease in severely immunodeficient NOD/SCID mice upon vaginal HSV-1 challenge but also protected animals even with neuronal HSV infection. We also report for the first time that an anti-gB specific monoclonal antibody prevents HSV-1-induced encephalitis entirely independently from complement activation, antibody-dependent cellular cytotoxicity, and cellular immunity. This indicates the potential for further development of MAb 2c as an anti-HSV drug.**

Herpes simplex virus (HSV) is a neuroinvasive human pathogen that critically depends on efficient infection of distinct target cells within a host. At the time of primary lytic infection, HSV replicates in peripheral mucocutaneous tissues and releases virions. A decisive characteristic of HSV infections in animals and humans is the establishment of a lifelong latency. HSV spreads from infected epithelial cells to axons of sensory neurons innervating the site of the primary infection, followed by retrograde transport to the respective dorsal root ganglia (12). Recurrent infections result from reactivation in neuronal cells, followed by virus replication and anterograde transport to cells at peripheral sites innervated by the respective neurons. Transmission between cells without diffusion through the extracellular environment represents a major route for HSV to spread between tissues and is thus a very efficient way for circumventing immunological barriers of the humoral immune response. Regardless of the dissemination pathway, however, fusion of the viral envelope with host membranes for delivery of the viral genome across the cellular lipid bilayer is essential for viral replication. In contrast to that of most other enveloped viruses, entry of herpesviruses into mammalian cells requires a multicomponent system and thus represents one of the most complex viral entry mechanisms studied so far. Among the 12 glycoproteins of the HSV envelope, glycoprotein B (gB), gD, and the gH/gL heterodimer display essential functions for both entry of extracellular virions and cell-to-cell spread. Binding of gD to one of its different cellular receptors, i.e., herpesvirus entry mediator (HVEM), nectin 1, or a modified form of heparan sulfate, promotes a conformational change of gD that subsequently triggers the fusogenic signal of the core fusion machinery, constituted in gB and gH/gL (36, 65).

The presence of the aforementioned glycoproteins both on the virion and on infected cells can be recognized by the immune system and elicits cellular and humoral immune responses. Recurrent HSV infections in the skin and mucosae appear to be controlled mainly by the host cellular immune response, such as T lymphocytes, macrophages, natural killer cells, and, as demonstrated recently, type I interferon (IFN)-producing plasmacytoid dendritic cells (10, 13, 15, 22, 29, 45, 47). High levels of preexisting neutralizing antibodies may play a role in preventing HSV spread and viremia. The reduction of neonatal HSV transmission in the presence of maternal HSV-specific antibodies underlines the protective effect of antibodies (8). In HSV-seropositive humans, circulating IgG antibod-

* Corresponding author. Mailing address: National Center for Tumor Diseases, Department of Medical Oncology, University of Heidelberg, D-69120 Heidelberg, Germany. Phone: 49-6221-56-37798. Fax: 49-6221-56-5373. E-mail: michaela.arndt@nct-heidelberg.de.

§ Present address: Institute of Virology, University Hospital Essen, University of Duisburg-Essen, 45147 Essen, Germany.

† Present address: Institute of Immunology and Genetics, 67655 Kaiserslautern, Germany.

▽ Published ahead of print on 1 December 2010.

ies are directed predominantly against gB and gD (9, 37). It has been shown that these antibodies act by antibody-dependent cellular cytotoxicity (ADCC) for efficient control of HSV infections in mice (31, 32, 44). High ADCC reactivity was also shown to positively correlate with protection against disseminated disease in human neonatal HSV infections (30, 33). Consistently, postexposure administration of human gamma globulin containing neutralizing HSV type 1 (HSV-1) antibodies or an anti-gD MAb to immunodeficient SCID or nude mice, respectively, prolonged survival but was not able to eventually protect animals from death (48, 60).

We previously isolated the gB-specific monoclonal antibody (MAb) 2c (17), which has potent HSV type 1 (HSV-1)-neutralizing activity *in vitro* and *in vivo* (18). In this study we showed that the efficiency of MAb 2c for neutralizing free HSV virions and inhibiting cell-to-cell spread is completely independent from ADCC, complement, and cellular effector mechanisms but critically relies on the antibody valency. Mapping of the MAb 2c epitope to the solved gB structure (25) suggests that the antibody interferes with HSV entry by blocking transmission of the fusogenic signal through cross-linking of gB trimers. We show that the bivalent MAb 2c is able not only to fully protect severely immunodeficient NOD/SCID mice from lethal viral challenge but also to rescue animals from lethal encephalitis even when the virus has reached the peripheral nervous system.

## MATERIALS AND METHODS

**Cells and viruses.** The hybridoma cell line secreting MAb 2c, generated from BALB/c mice hyperimmunized with HSV-1 strain 342 hv (17), was maintained either in Iscove's modified Dulbecco's medium (IMDM) with 10% fetal bovine serum (FBS), 100 U/ml penicillin, and 100 μg/ml streptomycin or in Ex-Cell hybridoma medium (Sigma-Aldrich, St. Louis, MO) supplemented with 10 mM L-glutamine (Invitrogen, Carlsbad, CA) for serum-free antibody production. The African green monkey kidney cell line Vero was obtained from the European Collection of Cell Cultures (ECACC) and grown in Dulbecco's modified Eagle's medium (DMEM) with 10% heat-inactivated FBS, 100 U/ml penicillin, and 100 μg/ml streptomycin. Experiments using Vero cells were performed in maintenance medium with 2% FBS. HSV-1 strain F and HSV-2 strain G were propagated in Vero cells, and titers were determined on Vero cells by the endpoint dilution assay as described previously (59) and expressed as 50% tissue culture infectious doses ($TCID_{50}$)/ml.

**Antibody production and purification.** MAb 2c (IgG2a) was purified from serum-free hybridoma supernatants by protein A chromatography (Thermo Scientific, Worcester, MA) and dialyzed against phosphate-buffered saline (PBS), and the purity was monitored on a calibrated Superdex 200 10/300 GL column (Amersham Pharmacia, Piscataway, NJ). Proteolytic digestion of MAb 2c to obtain $F(ab')_2$ and Fab fragments was carried out with a pepsin or papain preparation kit (Thermo Scientific) according to the manufacturer's instructions. Homogenous $F(ab')_2$ and Fab fragment preparations were obtained by immobilizing Fc fragments to a protein A column, followed by size exclusion chromatography of the flowthrough using a calibrated HiLoad 16/60 Superdex 200 preparative-grade column (Amersham Pharmacia). To generate a single-chain variable fragment (scFv), total RNA was isolated from $1 \times 10^7$ MAb 2c hybridoma cells using the RNA/DNA midikit (Qiagen, Valencia, CA), followed by mRNA preparation using the Oligotex mRNA minikit (Qiagen). The authentic 5′ ends of the MAb 2c variable heavy chain ($V_H$)- and the variable light chain ($V_L$)-encoding DNA sequences were amplified by 5′ rapid amplification of cDNA ends (RACE)-PCR using the Marathon cDNA amplification kit (BD Biosciences, Heidelberg, Germany) and the oligonucleotides IgG2a-CH1 and IgG2a-C-kappa, annealing to the 5′ constant regions of the heavy and light chains, respectively. Sequences of subcloned PCR gene products were verified by DNA sequencing. MAb 2c variable domains were subsequently amplified with deduced oligonucleotides specific to the 5′ end of the $V_H$ or $V_L$ chain gene and respective antisense primers. A standard $(Gly_4Ser)_3$ linker connecting the $V_H$ and $V_L$ domains was introduced by overlap extension PCR, and the 2c scFv was cloned into the bacterial expression plasmid pHOG21 (28). Periplasmic production and purification of the 2c scFv were carried out as described elsewhere (1). Concentrations of purified antibodies were determined spectrophotometrically from the absorbance at 280 nm using the extinction coefficients 1.43 for IgG, 1.48 for $F(ab')_2$, 1.53 for Fab, and 1.7 for scFv. Polyclonal human sera obtained from donors with high immunoglobulin titers for HSV-1 completely neutralized 100 $TCID_{50}$ of HSV-1 F at a dilution of 1:160.

**Determination of antibody affinity.** Monolayers of Vero cells were infected at 80 to 90% confluence with HSV-1 or HSV-2 at a multiplicity of infection (MOI) of 3 and harvested the next day by trypsinization followed by washing in PBS. Cell surface binding measurements of 2c antibodies were carried out as described previously (1). Briefly, purified MAb 2c or derived antibody fragments 2c $F(ab')_2$, 2c Fab, and 2c scFv were incubated in triplicate at concentrations of 0.03 nM to 500 nM with $5 \times 10^5$ Vero cells in 100 μl fluorescence-activated cell sorter (FACS) buffer (PBS, 2% FBS, 0.1% sodium azide) for 1 h at room temperature. Cells were washed twice with 200 μl FACS buffer and incubated with fluorescein isothiocyanate (FITC)-labeled Fab-specific goat anti-mouse IgG (15 μg/ml; Jackson ImmunoResearch, Newmarket, Suffolk, England) for detection of bound MAb 2c, 2c $F(ab')_2$, and 2c Fab. Bound scFv was detected by first incubating with saturating concentrations of the anti-c-myc MAb 9E10 (10 μg/ml; Roche, Indianapolis, IN), followed by two washes and incubation with Fcγ-specific FITC-labeled goat anti-mouse IgG (15 μg/ml; Jackson ImmunoResearch). Cells were washed twice and resuspended in FACS buffer. Fluorescence was measured on a FACSCalibur flow cytometer (BD Bioscience, San Jose, CA), and median fluorescence intensity (MFI) was calculated using the CellQuest software (BD Biosciences). Background fluorescence was subtracted, and equilibrium binding constants were determined by using the Marquardt and Levenberg method for nonlinear regression with GraphPad Prism version 4.0 (GraphPad Software, La Jolla, CA).

**Epitope characterization.** Immunoreactivity of MAb 2c with native or denatured truncated glycoprotein B [gB(730)t] (4), kindly provided by Roselyn J. Eisenberg and Gary H. Cohen (University of Pennsylvania, Philadelphia, PA), was determined essentially as described previously (4). Purified gB(730)t (0.75 μg) was resolved by 8% SDS-PAGE under either nonreducing (sample buffer containing 0.2% SDS) or denaturing (sample buffer containing 2% SDS and 155 mM β-mercaptoethanol, 2 min at 95°C) conditions and transferred onto a nitrocellulose membrane. Membrane strips were blocked with 2% milk in TNT buffer (0.1 M Tris-HCl [pH 7.5], 0.15 M NaCl, 0.05% Tween 20) for 1 h, followed by incubation with 5 μg/ml of glycoprotein B-specific antibodies MAb 2c, H126 (Novus Biologicals, Littleton, CO), and H1817 (Novus) in 2% milk–TNT buffer for 2 h at room temperature. Bound antibodies were detected with horseradish peroxidase-conjugated polyclonal goat anti-mouse antibody (1:20,000; QED Bioscience Inc. San Diego, CA) and chemiluminescence (Thermo Scientific,) using the LAS 3000 Luminescent Image Analyzer (Fujifilm, Tokyo, Japan).

COS-1 cells were transiently transfected by the DEAE-dextran method with plasmids coding for either the full-length HSV-1 gB (positions 31 to 904) (pRB9221) or C-terminal deletion mutants truncated at positions 720 (pTS690), 630 (pPS600), 503 (pRB9510), 487 (pRB9509), and 470 (pRB9508). The plasmids were kindly provided by L. Pereira (54, 57). Immunofluorescence assays with transfected cells using MAb 2c or control antibodies were carried out as described elsewhere (55).

**Peptide mapping.** Cellulose-bound overlapping 13-mer peptides and duotopes were automatically prepared according to standard SPOT synthesis protocols as described previously (21, 35) (JPT Peptide Technologies, Berlin, Germany). In addition, peptides coupled with a reactivity tag and a linker were immobilized chemoselectively on a modified glass surface in three identical subarrays and purified by removal of truncated and acetylated sequences by subsequent washing steps. Peptide microarrays were blocked with Tris-buffered saline (TBS) containing blocking buffer (Pierce International) for 2 h and incubated with 10 μg/ml MAb 2c in blocking buffer for 2 h. Peptide microarrays were washed with TBS containing 0.1% Tween (T-TBS), and peptide-bound antibody on the peptide membrane was transferred onto a polyvinylidene difluoride (PVDF) membrane. Anti-mouse IgG either peroxidase labeled (Sigma) or fluorescently labeled (Pierce) was used as the secondary antibody at a final concentration of 1 μg/ml in blocking buffer. After 2 h of incubation and final washing with T-TBS, PVDF membranes were analyzed using chemiluminescence substrate (Roche Diagnostics). Glass slide peptide microarrays were washed thoroughly with T-TBS and 3 mM SSC buffer (JPT Peptide Technologies), dried under nitrogen, and scanned using a high-resolution fluorescence scanner (Axon GenePix 4200 AL). Fluorescence signal intensities (light units [LU]) were analyzed using spot recognition software (GenePix 6.0) and corrected for background intensities from control incubations with secondary anti-mouse IgG.

**Virus neutralization assay.** Neutralizing activities of antibodies were determined by endpoint dilution assay as described previously (17). Briefly, serial dilutions of antibodies were incubated with 100 $TCID_{50}$ of HSV-1 or HSV-2 for 1 h at 37°C in cell culture medium. The antibody virus inoculum was applied to Vero cell monolayers grown in microtiter plates, and cytopathic effect (CPE) was scored after 72 h of incubation at 37°C. The antibody concentration required for reducing virus-induced CPE by 100% was determined as the complete neutralization titer. In addition, the virus neutralization capacity of monovalent 2c Fab fragments was investigated in the presence of cross-linking antibodies by adding an excess of anti-murine Fab IgGs (2,600 nM; Jackson ImmunoResearch, Newmarket, Suffolk, England) to the preincubation step. For control purposes, virus without antibody and antibody alone were used to induce maximal CPE and no CPE, respectively. Virus neutralization assays were repeated at least twice with similar results.

**Postattachment neutralization assay.** Prechilled (4°C for 15 min) Vero cell monolayers were infected with 100 $TCID_{50}$ HSV-1 F at 4°C for 1 h to allow virus absorption before serial dilutions of either MAb 2c or a polyvalent IgG preparation from human plasma (Intratect; Biotest AG, Dreieich, Germany) were added (postattachment neutralization). To compare the preattachment versus postattachment neutralization efficacy of MAb 2c under identical experimental conditions, 100 $TCID_{50}$ HSV-1 F were incubated for 1 h at 4°C with the same antibody dilutions before being added to prechilled Vero cell monolayers. Inoculated Vero cells from both assays were incubated for another 1 h at 4°C before being transferred to 37°C. Neutralization titers were determined after 72 h as described above for the standard neutralization assay.

**Cell-to-cell spread assay.** Confluent monolayers of Vero cells, grown either on glass coverslips for immunofluorescence studies or in 24-well tissue culture plates for analysis by light microscopy, were infected with either HSV-1 F or HSV-2 G. After 4 h of adsorption at 37°C, the virus inoculum was removed and cells were incubated in DMEM containing 2% FBS in the presence of neutralizing antibodies, pooled human sera derived from immunized donors with high titers of anti-HSV-1 immunoglobulins (1:20), or medium alone as positive control. At 48 h postinfection, cells were fixed with 4% paraformaldehyde for immunostaining or analyzed directly for plaque formation under a Zeiss Observer Z1 light microscope at a 50-fold magnification. To visualize the viral spread by indirect immunofluorescence, cells were rinsed twice with PBS, incubated for 15 min in 500 μl HEPES-buffered saline with 0.05% Tween 20, and stained with FITC-conjugated polyclonal goat anti-HSV serum (1:100; Bethyl, Montgomery, TX). Stained cells washed three times with PBS were mounted in mounting medium containing 0.2 g/ml Mowiol 4-88 (Calbiochem, San Diego, CA). Immunofluorescence images were acquired with a Leica DM IRE2 confocal microscope at a 40-fold magnification. Cell-to-cell spread inhibition was tested in addition by postadsorption virus neutralization assay. Vero cells grown to confluence in six-well plates were incubated for 4 h at 37°C with 200 $TCID_{50}$ of HSV-1 F in 3 ml DMEM containing 2% FBS and antibiotics. Cell monolayers were washed twice with PBS and overlaid with warm plaquing medium (DMEM, 5% [wt/vol] agarose, 10% FBS, and antibiotics) containing an excess of neutralizing antibodies or polyclonal human HSV-1-neutralizing sera. Plaque formation was analyzed by light microscopy after 48 h of incubation at 37°C.

**DNA quantification.** HSV-1 and HSV-2 genomes were quantified by real-time PCR. DNA was purified from samples containing equivalent amounts of infectious particles of HSV-1 and HSV-2 using the MagNA Pure LC automated nucleic acid extraction system (Roche) according to the manufacturer's instructions. Viral DNA was then quantified by real-time PCR (LightCycler; Roche) using the RealArt HSV-1/HSV-2 quantification kit (Qiagen).

**Mouse protection experiments.** Anesthetized female nonobese diabetic/severe combined immunodeficient (NOD/SCID) mice (NOD.CB17-*Prkdc*$^{scid}$/J; Charles River Laboratories, Research Models and Services, Sulzfeld, Germany), 6 to 8 weeks of age, were challenged intravaginally with a 20-μl inoculum of $1 \times 10^6$ $TCID_{50}$ HSV-1 F per mouse. Skin glue (Epiglu; Meyer-Haake Medical Innovations, Wehrheim, Germany) was applied to the vulva to prevent discharge of the virus inoculum. The delivered inoculum induced infection rates of >94% as assessed by culture of vaginal lavage. Mice were examined daily after viral inoculation for loss of weight, vulvitis/vaginitis (redness, mucopurulent discharge, and signs of inflammation), and neurological disease. Mice displaying any of these symptoms were sacrificed immediately. Mice were passively immunized by intravenous (i.v.) injection of purified MAb 2c either 24 h prior to viral inoculation for immune prophylaxis or 24 h, 40 h, and 56 h after viral infection for therapeutic treatment. Mice were assessed for infection by determination of virus titers from vaginal irrigations obtained on days 1, 2, 4, 6, and 8 after infection and at the time of death using the endpoint dilution assay on Vero cells. Viral loads in organs (spleen, adrenal gland, lung heart, liver, kidney, spinal cord, and brain) of sacrificed mice were determined after homogenization of organs by titration on Vero cell monolayers as described elsewhere (42). Each test and control group contained 9 or 10 animals with detectable HSV-1 infection.

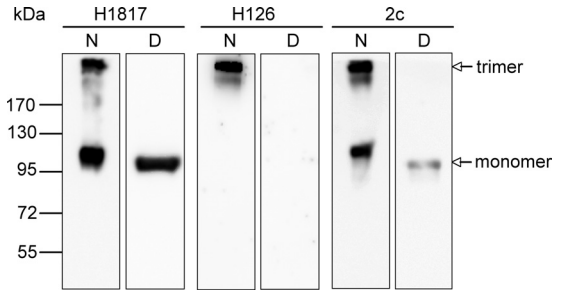


FIG. 1. Characterization of MAb 2c according to its reactivity with gB under different SDS-PAGE conditions. Recombinant gB(730)t resolved by SDS-PAGE under either nonreducing, native (N) or reducing, denatured (D) conditions was transferred to nitrocellulose membranes and probed with gB-specific monoclonal antibody H1817, H126, or 2c. For controls, MAbs H1817 and H126, recognizing a continuous epitope and a discontinuous epitope, respectively, were used. Molecular mass is indicated on the left and migration of gB trimer and monomer on the right.

## RESULTS

**Mapping and analysis of the gB epitope recognized by MAb 2c.** The recently determined crystal structure of the ectodomain of gB from HSV-1 revealed a multidomain trimer with five distinct structural domains: domain I (base), domain II (middle), domain III (core), domain IV (crown), and domain V (arm) (25). To characterize the neutralizing epitope of MAb 2c, we tested its reactivity with recombinant gB(730)t (4) in Western blot analysis under either reducing or nonreducing conditions. As controls, we used MAb H1817, recognizing a linear epitope (4), and MAb H126, recognizing a discontinuous epitope (34). A typical staining pattern for a linear epitope was obtained in Western blot analysis with MAb H1817, showing detection of monomeric and trimeric forms of gB under nonreducing conditions and sole predominant staining of gB monomer under reducing conditions (Fig. 1). As expected, MAb H126 reacted with gB only under native conditions. Surprisingly, recognition of solely the upper gB protein band of >170 kDa suggests that MAb H126 is trimer specific (Fig. 1). MAb 2c reacted with native and denatured gB; however, reactivity under denaturing conditions was much weaker than with MAb H1817 (Fig. 1). Weak reactivity with gB monomers under denaturing conditions has been previously reported for a set of other neutralizing antibodies binding to discontinuous epitopes that seem either to be resistant to denaturation or to refold during SDS-PAGE and therefore are termed "pseudo-continuous" epitopes (4).

To narrow down the identity of the conformation-dependent epitope, reactivity of MAb 2c was further characterized using COS-1 cells transiently transfected with plasmids encoding either full-length gB (positions 31 to 904) or gB mutants with C-terminal truncations at positions 720, 630, 503, 487, and 470. The shortest gB deletion mutant showing positive internal immunofluorescence signals was truncated at position 487 (data not shown). Thus, we reasoned that the epitope for MAb 2c is located within residues 31 to 487.

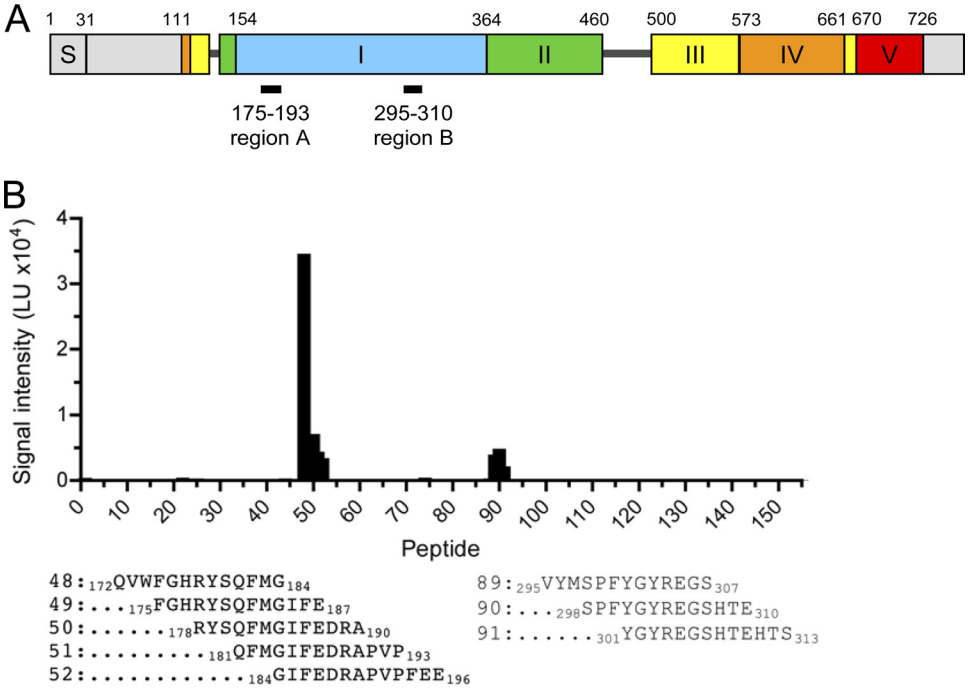


FIG. 2. Peptide mapping of MAb 2c to gB. (A) Schematic localization of binding regions A and B identified on a peptide library spanning the extracellular domain of gB from amino acid 31 to 505. The 13-mer peptides were synthesized on a continuous cellulose membrane with an offset of 3 amino acids, and bound MAb 2c was detected with a peroxidase-conjugated secondary antibody by chemiluminescence. Coloring of functional domains I to V corresponds to the crystal structure of gB reported by Heldwein et al. (25), and regions not solved in the crystal structure are shown in gray (25), S, signal sequence. (B) Fluorescence signal intensities from high-resolution laser scans with 13-mer peptides immobilized on glass slides via a flexible linker.

To identify the specific epitope involved in binding of MAb 2c, we used gB-derived peptides displayed on peptide microarrays. First, the gB sequence displaying amino acids 31 to 505 was prepared by SPOT synthesis as overlapping 13-mer peptides bound with uncharged acetylated amino-terminal ends to a continuous cellulose membrane with an offset of 3 amino acids. To avoid shifting of the binding equilibrium for the noncomplexed antibody, MAb 2c peptide scans were immobilized on a PVDF membrane prior to detection by chemiluminescence. As shown in the schematic representation of the full-length gB with indicated functional domains (Fig. 2A), MAb 2c reactivity was restricted to peptides spanning two separate regions within domain I, i.e., three consecutive peptides comprising residues 175 to 193 (binding region A) and two overlapping peptides comprising residues 295 to 310 (binding region B). To validate the identified binding regions, we used an additional set of purified 13-mer peptides immobilized on glass slides via a flexible linker. Compared to the cellulose screen, the readout of this microarray scanning via fluorescence confirmed the same epitope binding regions (Fig. 2B). Due to the application of purified peptides and a high-resolution microarray scanning system, additional consecutive peptides at both binding sites were recognized by MAb 2c in this peptide microarray (Fig. 2B).

We mapped the identified binding sites for MAb 2c to the solved gB structure (25). Interestingly, the peptide $_{172}$QVWF GHRYSQFMG$_{184}$, showing the strongest reactivity with MAb 2c, overlapped with one of the two putative fusion loops (fusion loop 1, $_{173}$VWFGHRY$_{179}$) located in a curving subdomain of domain I (23) (Fig. 3). However, localization of binding site A at the base of the gB trimer makes it inaccessible to MAb 2c in the available gB structure most likely representing the postfusion conformation (25). Residues of binding site B are exposed and located at the upper part of domain I (Fig. 3).

To further assess the conformation-dependent epitope of MAb 2c, consensus sequences of both binding regions were connected in various combinations as duotopes either directly or separated by one or two β-alanine spacers (Fig. 4). It has recently been shown that linker insertions in close proximity to fusion loop 1 after residue $E_{187}$ result in fusion-deficient gB mutants (41), even though gB folds into a postfusion conformation (41). Therefore, we included in addition to the consensus motif $_{179}$YSQFMG$_{184}$ of binding region A the $_{186}$FED$_{188}$ motif of binding region A into separate duotope scans. Compared to the peptide $_{172}$QVWFGHRYSQFMG$_{184}$, displaying the strongest binding reactivity with MAb 2c in the 13-mer peptide scans (Fig. 4), the combination of both binding site A motifs with the consensus peptide $_{300}$FYGYRE$_{305}$ of binding site B resulted in two duotopes with enhanced signal intensities (Fig. 4, duotope sets I and II). Whereas the strength of binding of MAb 2c to duotope $_{179}$YSQFMG$_{184}$-βA-$_{300}$FYGYRE$_{305}$ was only slightly increased, near saturation of the fluorescence signal intensity was obtained with duotope $_{186}$FED$_{188}$-βA-βA-$_{300}$FYGYRE$_{305}$.

Thus, the results from the peptide microarrays correspond to the Western blotting results and demonstrate that MAb 2c recognizes a conformation-dependent epitope. To prevent fusion of the virion envelope with the cell membrane, MAb 2c

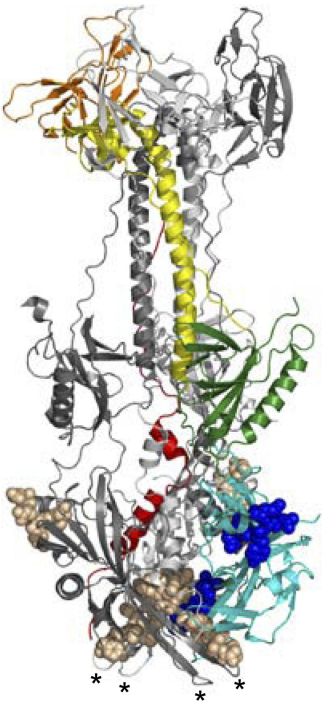

FIG. 3. Localization of neutralizing MAb 2c epitopes on the gB crystal structure (Protein Data Bank [PDB] accession no. 2GUM). The ribbon diagram of the gB trimer shows one protomer with functional domains colored (domain I in cyan, domain II in green, domain III in yellow, domain IV in orange, and domain V in red). The other two protomers are shown in dark and light gray. Asterisks indicate the fusion loops of protomers highlighted in gray; fusion loops of the colored protomer are not visible. The mapped residues of the discontinuous MAb 2c epitope, $F_{175}$ to $A_{190}$ and $F_{300}$ to $E_{305}$, are indicated in surface representation by dark blue for the color-coded protomer and by rose for both other protomers.

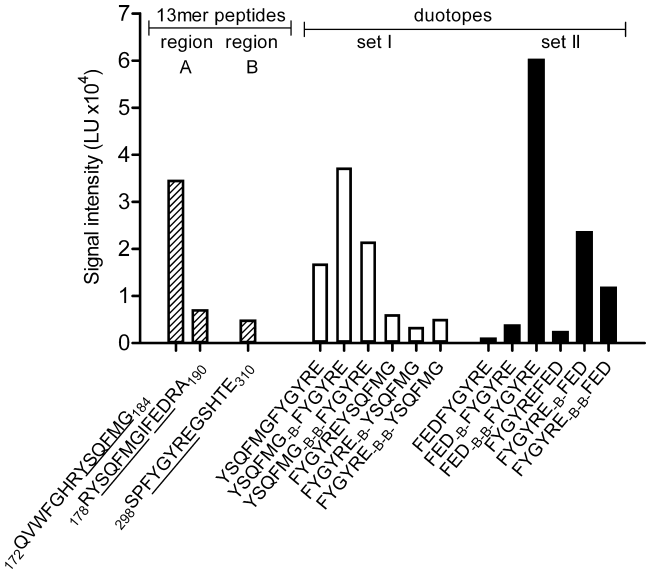


FIG. 4. Duotope scanning of MAb 2c. Consensus sequences (underlined) of MAb 2c binding regions A and B (dashed bars) were synthesized as duotopes (white and black bars) either joined directly or separated by one or two β-alanine spacers (B and B-B). The reactivity of MAb 2c with duotopes was recorded by fluorescence signal intensities from high-resolution laser scans.

should bind to the prefusion conformation of gB. However, the neutralizing epitope of MAb 2c maps only in part to the surface of the gB conformation present in the available gB crystal structure (25), which indicates that gB might adopt distinct conformations during entry.

**Characterization of MAb 2c-derived bivalent and monovalent antibodies.** Monoclonal antibodies have been used by several investigators to identify regions on gB that are essential for its function in virus entry (4, 26, 40, 54). It has been suggested that neutralizing antibodies, which have been mapped to a unique functional region at the base of the gB trimer comprising residues of the C-terminal end of domain V and residues of domain I of a proximate protomer, interfere with the fusogenic activity of gB (4). We therefore hypothesized that monovalent antibody binding to the MAb 2c epitope within domain I close to the C terminus of domain V should sufficiently block cooperative conformational changes upon activation of gB. Since MAb 2c neutralizes HSV-1 without complement *in vitro* (17), we generated conventional $F(ab')_2$ and Fab fragments and a recombinant single-chain variable fragment (scFv) as valuable tools for studying the hypothesized mechanism mediated by MAb 2c. The homogeneity of the generated antibody preparations was monitored by size exclusion chromatography (data not shown).

Flow cytometry analysis using Vero cells either infected or not infected with HSV-1 or HSV-2, respectively, demonstrated specific binding of MAb 2c and MAb 2c-derived antibody fragments (data not shown). We further used fluorescence cytometry to determine equilibrium binding curves of the antibodies to HSV-1- and HSV-2-infected Vero cells (Fig. 5). The results of these studies demonstrated higher apparent affinities for the whole IgG and the $F(ab')_2$ fragment than for the Fab and scFv, respectively (Table 1). The increment in functional affinity (avidity) for the bivalent antibodies relative to the determined affinities of the monovalent antibodies indicates that the bivalent antibodies were able to bind two gB epitopes on the cell surface simultaneously. Bivalent MAb 2c and 2c $F(ab')_2$ showed a 1.7- to 2.8-fold-higher apparent affinity than their monovalent counterparts. The slight increment in the apparent affinity of the $F(ab')_2$ fragment versus the IgG might be due to the higher flexibility of the antigen binding sites within the $F(ab')_2$ construct. The similar apparent affinities of MAb 2c, 2c $F(ab')_2$, and 2c Fab for both HSV-1- and HSV-2-infected Vero cells confirmed that the recognized gB epitope does not structurally differ between the two viruses (Table 1).

**Neutralization activities of monovalent and bivalent antibodies *in vitro*.** The equal neutralization efficacy of MAb 2c irrespective of whether the antibody was added before (preattachment) or after (postattachment) HSV-1 virions interacted with Vero cells (Fig. 6A) indicated that MAb 2c does not interfere with virus binding to target cells. In contrast, the polyclonal human gamma globulin Intratect clearly neutralized by inhibition of virion attachment to target cells (Fig. 6B). The neutralizing activities of MAb 2c-derived fragments $F(ab')_2$, Fab, and scFv were compared with that of their parental IgG counterpart in a standard neutralization assay on Vero cells. The parental MAb 2c reduced HSV-1-induced cytopathic ef-

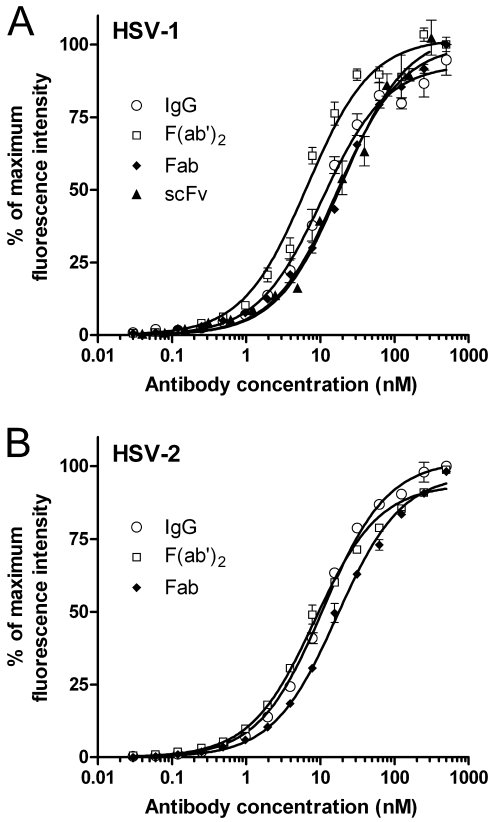


FIG. 5. Equilibrium binding curves for MAb 2c, 2c F(ab′)$_2$, 2c Fab, and 2c scFv as determined by flow cytometry. Binding activities to HSV-1 F (A)- or HSV-2 G (B)-infected Vero cells at the indicated concentrations are shown as percentage of maximum median fluorescence intensity. Experiments were twice performed in triplicate; error bars represent standard deviations.

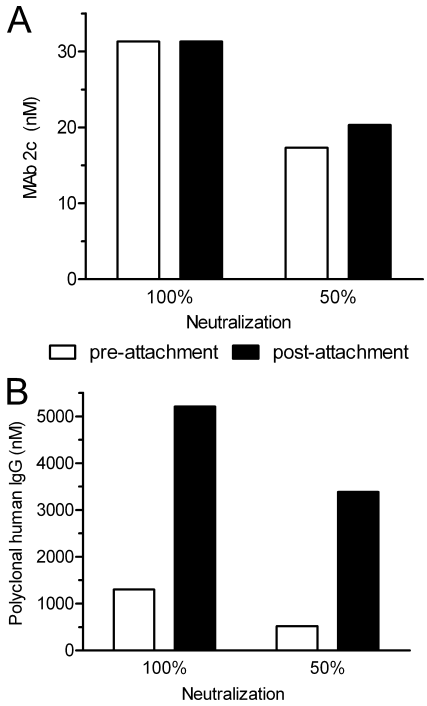


FIG. 6. Inhibition of HSV-1 virion attachment to target cells by MAb 2c. Serial dilutions of MAb 2c (0.98 to 125 nM) (A) or polyvalent human gamma globulin (Intratect) (0.33 to 42 μM) (B) were added to Vero cell monolayers in 96-well microtiter plates following preincubation with 100 $TCID_{50}$ HSV-1 (preattachment neutralization) or postadsorption of 100 $TCID_{50}$ HSV-1 to target cells (postattachment neutralization). The highest antibody titer and polyvalent human IgG titer, respectively, preventing virus-induced cytopathic effect (CPE) in 10 individual inoculated cell monolayers to 100% and 50% relative to controls were determined after 72 h of incubation at 37°C and considered the endpoint. Standard errors of the means from three independent experiments were <0.1.

fect (CPE) by 100% at a concentration of 8 nM. Interestingly, a 4-fold-higher MAb 2c concentration was required to completely reduce HSV-2-induced CPE (Fig. 7A). The bivalent 2c F(ab′)$_2$ reduced both HSV-1- and HSV-2-induced CPE twice as efficiently as the parental MAb 2c. Surprisingly, we observed a fundamental difference in the abilities of the monovalent 2c antibody fragments to neutralize HSV-1 and HSV-2. Compared to the parental MAb 2c, approximately 375- and 94-fold-higher concentrations of 2c Fab were necessary to reduce HSV-1- and HSV-2-induced CPE by 100%, respectively (Fig. 7A). The recombinant 2c scFv showed a plaque-reductive effect under the light microscope but was not able to reduce HSV-induced CPE by 100% even at the highest tested concentration of 3,000 nM (data not shown).

TABLE 1. Apparent equilibrium constants for binding of MAb 2c and derived antibody fragments to HSV-1 F- or HSV-2 G-infected Vero cells

| Virus | $K_D$ (nM)-[a] | | | |
|---|---|---|---|---|
| | IgG (bivalent) | F(ab′)$_2$ (bivalent) | Fab (monovalent) | scFv (monovalent) |
| HSV-1 F | 10.2 | 6.9 | 17.3 | 19.2 |
| HSV-2 G | 10.7 | 8.8 | 17.7 | ND |

[a] Equilibrium constants ($K_D$s) for binding to gB on HSV-infected cells were determined by fitting the data from the equilibrium binding curves determined by flow cytometry (Fig. 5) to the Marquardt-Levenberg equation. ND, not determined.

Since both bivalent antibodies MAb 2c and 2c F(ab′)$_2$ neutralized HSV-2 about four times less effectively than HSV-1 (Fig. 7A), we analyzed the genome copy numbers of HSV-1 and HSV-2 preparations containing equal amounts of infectious particles by quantitative real-time PCR. Compared to HSV-1, a 4-fold-higher number of genome equivalents was found for HSV-2 (data not shown), correlating well with the higher antibody titers of MAb 2c and 2c F(ab′)$_2$ required for HSV-2 neutralization.

Neutralization assays as shown in Fig. 7A indicated a strong correlation between antibody valency and neutralization efficiency. Consequently, we investigated whether the ability of 2c Fab fragments for clearing virus infection could be restored by cross-linkage of the Fab fragments. The virus neutralization assay was repeated for 2c Fab in the absence or presence of IgGs reacting with murine Fab fragments. As shown in Fig. 7B, cross-linking of 2c Fab dramatically increased neutralizing activity but could not restore it to the same efficacy as for the parental MAb 2c. Anti-murine Fab IgGs alone showed no effect on virus neutralization (data not shown).

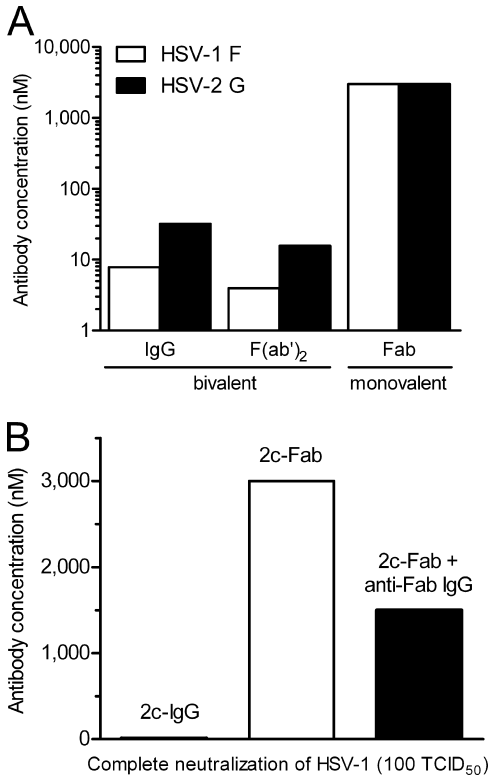


FIG. 7. Effect of valency of anti-gB antibodies on *in vitro* neutralization of HSV. (A) Bivalent antibodies MAb 2c (IgG) and 2c F(ab′)$_2$ and monovalent 2c Fab were incubated in serial dilutions for 1 h with 100 $TCID_{50}$ HSV-1 F or HSV-2 G before inoculation onto Vero cells. CPE was scored 72 h later as described in the legend to Fig. 6. Shown are antibody concentrations required to neutralize 100% of the viral inoculum from one of three representative replicate experiments. (B) Antiviral activity of 2c Fab fragments cross-linked with murine anti-Fab IgGs.

**Inhibition of cell-to-cell spread.** Despite the ability of gB- and gD-specific monoclonal antibodies to neutralize HSV-1 with high efficacy, some of them failed to protect cells from viral spread in tissue culture (11, 50). We therefore first compared the efficacies of MAb 2c for inhibiting cell-to-cell spread of HSV-1 and HSV-2 in a plaque reduction assay. As shown in Fig. 8, a concentration-dependent reduction of plaque size by MAb 2c was observed for both HSV serotypes. At a concentration of 500 nM, MAb 2c completely abolished HSV-1 plaque development (Fig. 8A). Similar to the results of the neutralization experiments, a 4-fold-higher MAb 2c concentration was required to also completely inhibit cell-to-cell transmission in HSV-2 infected cells (Fig. 8B).

Although 2c Fab fragments did not efficiently neutralize free virions but it was reported that small antibody fragments may exhibit more favorable diffusion properties (68), we investigated their activity for preventing HSV-1 from crossing cell junctions from infected to uninfected cells. For this analysis, we employed a more sensitive immunofluorescence assay. Both bivalent antibodies, MAb 2c and 2c F(ab′)$_2$, completely abrogated HSV-1 spread in Vero cell monolayers, and only single infected cells could be visualized by indirect immunofluorescence (Fig. 9). Despite the ability of the polyclonal human serum to neutralize free virions, it completely failed to inhibit viral cell-to-cell spread. This is most likely the result of the heterogeneous population of neutralizing antibodies directed against numerous HSV epitopes. Compared with polyclonal human immune serum, the monovalent 2c Fab fragment was able to control cell-to-cell spread to some extent. In contrast to its bivalent counterparts, however, the monovalent 2c Fab fragment was not able to completely abrogate viral spread even when tested at a 6-fold-higher concentration (Fig. 9). Hence, antibody valency played a key role in also inhibiting spread of HSV-1 between adjacent cells.

**Immunoprotection of immunodeficient mice against disseminated HSV infection.** We showed previously that mice depleted of both $CD4^+$ and $CD8^+$ T cells were fully protected from lethal encephalitis by passive transfer of MAb 2c after intravaginal HSV-1 infection (18). Natural killer (NK) cells accumulating at the site of HSV-2 infection in humans (29) are the early source of gamma interferon (46), which plays an essential role in the control of HSV infection (2, 46, 64). More recently, it has been demonstrated for the first time that human NK cells mediate protection against primary genital HSV

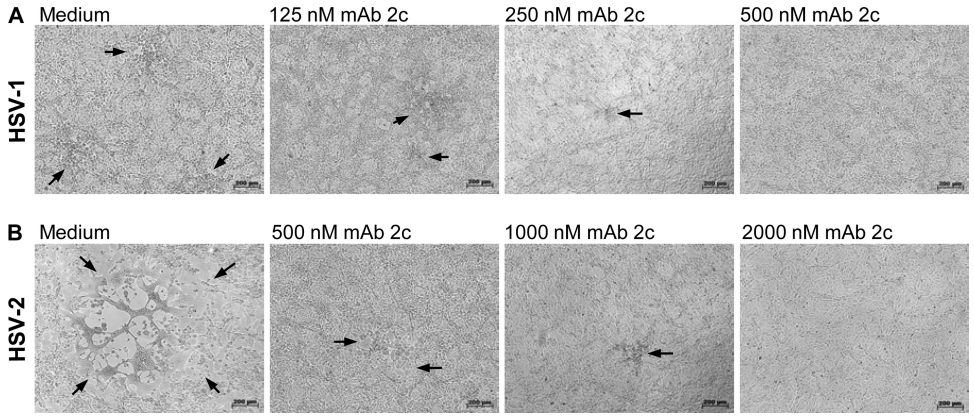


FIG. 8. Inhibition of cell-to-cell spread of HSV-1 and HSV-2 on Vero cell monolayers by MAb 2c. Vero cell monolayers infected with 100 $TCID_{50}$/500 μl of HSV-1 (A) and HSV-2 (B) were treated with increasing concentrations of MAb 2c as indicated. The concentration-dependent plaque reduction on Vero cell monolayers is shown by light microscopy after 48 h of incubation. The microscopic pictures shown are representative of multiple image sections observed in two independent experiments. Bar, 200 μm.

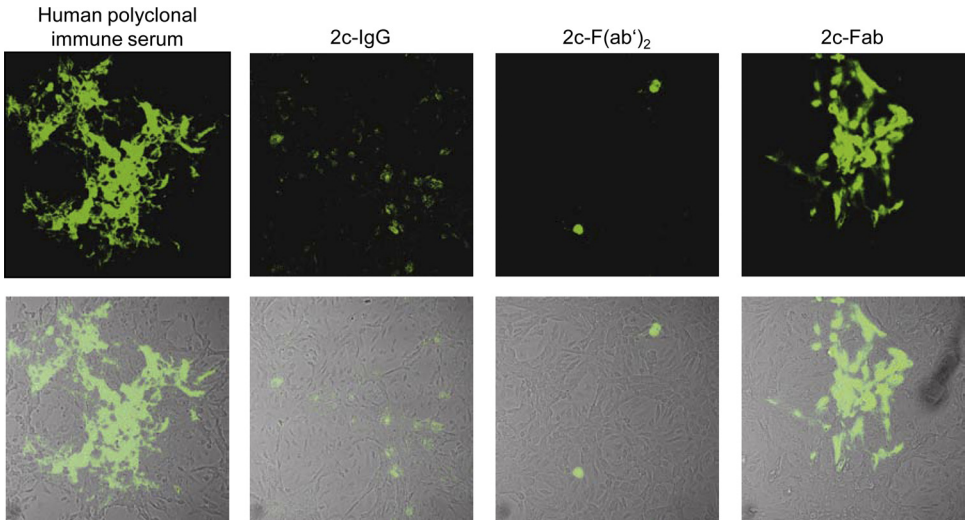


FIG. 9. Inhibition of HSV-1 cell-to-cell spread. Immunofluorescence (upper panel) and overlays of light microscopy and immunofluorescence pictures (lower panel) of confluent Vero cell monolayers 48 h after infection with HSV-1 (400 $TCID_{50}$/500 μl) treated with pooled human polyclonal HSV-1-neutralizing sera (1:20), MAb 2c (IgG, 500 nM), 2c $F(ab')_2$ (500 nM), or 2c Fab (3,000 nM) are shown. Viral antigens were visualized by immunostaining with FITC-conjugated polyclonal goat anti-HSV serum. Uninfected cells (mock) used as a control showed no background staining (not shown).

infection in humanized mice as an innate immune response (38). To investigate whether MAb 2c confers antiviral activity independently of an antibody-mediated immune response, we employed a NOD/SCID mouse model, which in addition to the SCID T- and B-cell deficiency, lacks NK cell and macrophage function and the ability to stimulate the complement pathway. Intravaginal HSV-1 infection ($1 \times 10^6$ $TCID_{50}$) of NOD/SCID mice resulted in rapid progressive systemic disease with a median survival time of 9 days. HSV titers in organs were determined by an endpoint dilution assay, showing high viral titers in spinal cord ($2.3 \times 10^6$ $TCID_{50}$), brain ($3.8 \times 10^5$ $TCID_{50}$), and vaginal mucosa ($1.4 \times 10^6$ $TCID_{50}$), moderate titers in kidney ($1.7 \times 10^4$ $TCID_{50}$) and adrenal glands ($1.1 \times 10^4$ $TCID_{50}$), and low titers in lung ($1.1 \times 10^3$ $TCID_{50}$) and heart ($1.9 \times 10^2$ $TCID_{50}$) (data not shown). To assess the therapeutic efficiency of MAb 2c, NOD/SCID mice were treated intravenously with either 2.5 mg/kg, 5 mg/kg, or 15 mg/kg of antibody at 24 h prior to intravaginal HSV-1 challenge (Fig. 10). Mice receiving the low antibody doses were not fully protected against lethal infection by HSV-1. Median survival times of mice treated with 5 mg/kg MAb 2c, however, were 2.6-fold-longer than those of control mice receiving PBS. The HSV-1 titers in the investigated organs from mice not protected against lethal encephalitis were comparable to those in the untreated control group. In contrast, full protection of animals was achieved at a dose of 15 mg/kg MAb 2c. Viral titers in organs of mice protected by the antibody were below the detection limit of $1 \times 10^2$ $TCID_{50}$.

We next evaluated whether postexposure immunization with MAb 2c also confers protection from viral dissemination and lethal encephalitis in the presence of an established peripheral HSV infection. NOD/SCID mice with high HSV-1 titers in vaginal irrigations at 24 h after viral challenge were repeatedly treated at 24 h, 40 h, and 56 h intravenously with 15 mg/kg of MAb 2c (Fig. 11A and B). The PBS-treated control group showed constant vaginal virus shedding until mice with neurological symptoms had to be sacrificed at between day 7 and day 9. In contrast, MAb 2c cleared established HSV-1 infection by day 8 and completely prevented lethal outcome of infection ($3 \times 300$ μg; $P = 0.0003$ compared with PBS). Furthermore, no virions were detected in sensory neurons and organs of MAb 2c-treated animals at 1 month after infection (data not shown).

## DISCUSSION

Following the steps viruses take to enter target cells, virus-neutralizing MAbs can inhibit entry by several mechanisms. The specific interaction of viral surface proteins with cellular proteins, lipids, or carbohydrates represents the initial stage of infection, which can be blocked by neutralizing antibodies.

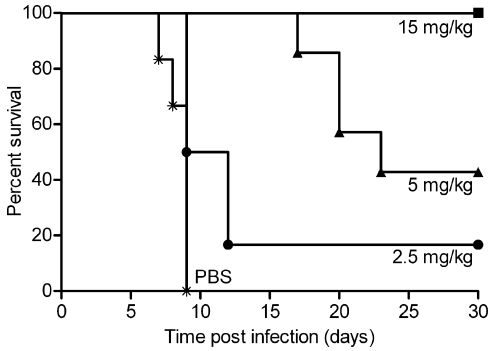


FIG. 10. Dose-dependent survival of MAb 2c-treated immunodeficient mice. NOD/SCID mice received different single dosages of MAb 2c intravenously 24 h before intravaginal challenge with $1 \times 10^6$ $TCID_{50}$ HSV-1 ($n = 7$ animals per group for PBS; $n = 9$ for all other groups).

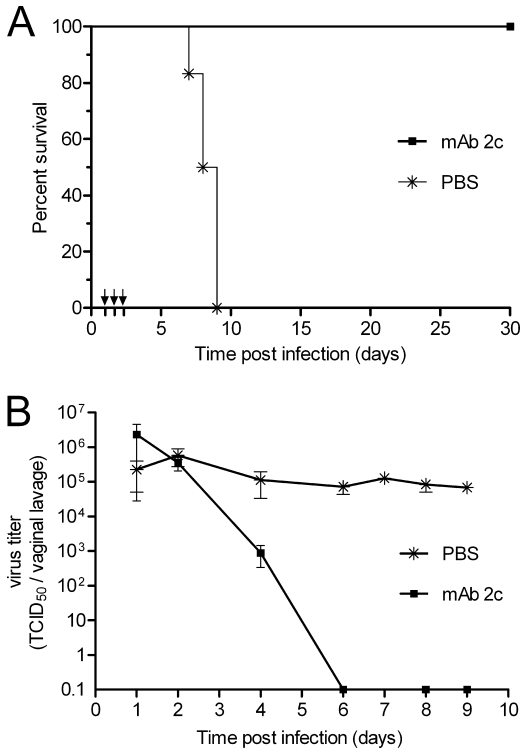


FIG. 11. Protection of NOD/SCID mice against HSV-1 dissemination by systemically applied MAb 2c. (A) Starting at 24 h postinfection, mice received 15 mg/kg MAb 2c three times intravenously at the time points indicated by arrows (24 h, 40 h, and 56 h). (B) Vaginal virus titers of MAb 2c- or control-treated mice were determined from vaginal irrigations cultured on Vero cell monolayers. Error bars indicate standard deviation ($n = 6$ infected animals per group for PBS; $n = 9$ for MAb 2c).

Antibodies inhibiting virus attachment either directly bind to the virion receptor binding site, as in the case of MAb F105 reacting with the CD4 binding site of HIV-1 gp120 and Fab HC19 covering the receptor binding site of influenza virus hemagglutinin (HA) (6, 20, 56), or sterically interfere with receptor engagement, as in the case of Fab HC45 binding in 17-Å proximity to the HA receptor binding site (19). In addition to the essential binding of HSV gD to one of its cellular receptors, gB plays a role in virion attachment to target cells. Recently, the existence of two heparan sulfate proteoglycan-independent true cell surface receptors and/or attachment factors for HSV gB has been described (5, 24, 62). Paired immunoglobulin-like type 2 receptor (PILRα) has been characterized as one possible protein receptor of gB, at least in certain cell types (62). For MAb 2c, comparative pre- versus postattachment neutralization assays showed that the antibody may not inhibit binding of virus to the cell surface but that it blocks viral entry. It has been shown previously that the interaction of gB with lipid membranes via key hydrophobic and hydrophilic residues of its fusion domain (23, 24) can be blocked by MAbs that recognize epitopes in close proximity to the fusion loops (4, 23). Because the conformational epitope of MAb 2c partially overlaps with fusion loop 1, we reasoned that binding of MAb 2c most likely interferes with transmission of the fusogenic signal, and we further evaluated neutralization at the postbinding/prefusion stage as a possible mode of action.

Triggered structural rearrangement is a key feature of viral fusogenic glycoproteins, resulting in distinct prefusion and postfusion conformations. Epitopes of different neutralizing MAbs have been mapped along the lateral domains of the spikes and to the tip of the crown of the gB crystal structure (4, 25). The epitope of MAb 2c maps to a unique functional region (FR1) at the base of the gB trimer consisting of residues within the C-terminal helix αF of domain V and residues within domain I of a proximate protomer (4). Our homology model shows that one part of the discontinuous epitope ($F_{300}$ to $E_{305}$) recognized by MAb 2c localizes to the upper section of domain I of gB, which has characteristics of a pleckstrin homology (PH) domain (7, 39). The other part of the epitope ($F_{175}$ to $A_{190}$, also located in domain I), however, is buried and would be inaccessible to MAb 2c binding unless gB undergoes a major conformational change. We therefore hypothesized that MAb 2c impedes transition of gB preferentially in the prefusion conformation. Based on the MAb 2c epitope localization and the assumption that conformational changes upon activation are cooperative, we reasoned that monovalent interaction of MAb 2c would be sufficient for blocking juxtaposition of the fusogenic domain of gB and the cellular membrane. Surprisingly, however, none of the generated monovalent antibody fragments (Fab and scFv) was able to efficiently neutralize free virions or to inhibit viral cell-to-cell spread. In contrast, both bivalent molecules, MAb 2c and 2c F(ab′)$_2$, were highly effective for virus neutralization and cell-to-cell spread inhibition. Retention of specific and comparable binding activities of all MAb 2c-derived antibodies in this study excludes functional differences of monovalent and bivalent antibodies due to impaired antigen recognition. Multivalent binding of immunoglobulins augments their functional affinity (27). The gain in functional affinity, however, inversely correlates with the intrinsic affinity of the antibody binding site (51). The only-moderate increment in equilibrium constants of between 1.7 and 2.8 for the bivalent 2c antibodies, IgG and F(ab′)$_2$, compared to their monovalent counterparts, scFv and Fab, is thus not unusual for antibodies with intrinsic affinities in the low-nanomolar range. Thus, the higher apparent affinity in fact indicates that multivalent (higher-avidity) binding to the gB antigen does occur and suggests that the antiviral activity of MAb 2c and 2c F(ab′)$_2$ is a consequence of gB cross-linking. Inferior neutralization efficiency of monovalent versus bi- or multivalent antibodies with specificity for the gH antigen of varicella-zoster virus (VZV) has been discussed as a matter of steric hindrance due to the different sizes of these antibodies (16). Although we cannot completely exclude this possibility as a potential additional neutralization mechanism for the MAb 2c variants, this seems unlikely because a direct correlation between antibody size, neutralization efficiency, and cell-to-cell spread inhibition was not observed. Furthermore, our data show that the smaller 2c F(ab′)$_2$ had an even better virus neutralization activity than the larger 2c IgG. Hence, the present observations indicate that gB cross-linking is the key mechanism for the antiviral activity of MAb 2c and suggest that stabilization of the gB prefusion conformation through immobilization of gB trimers inhibits activation of the fusogenic signal. A recent study by Silverman et al. (63) proposed that a

fusion-deficient phenotype of the HSV-1 gB ectodomain upon insertion of five amino acids after residue $E_{187}$ close to the fusion loop 1 may result not from interference with conformational changes of gB but rather from interference with other mechanistic gB functions. In our duotope scans MAb 2c reacted most strongly with binding site A/B duotope $_{186}$FED$_{188}$-βA-βA-$_{300}$FYGYRE$_{305}$, covering the particular insertion site $E_{187}$, which seems to be critical for gB function. It is therefore tempting to speculate that MAb 2c cross-linking impairs the ability of gB to interact with the other components of the HSV fusion machinery. However, further research is necessary, since our results do not allow us to distinguish whether cross-linking blocks the conformational change of gB itself or blocks the interaction between gB, gD, and gH/gL, which occurs during cell fusion (3) and is essential for completing the fusion process (67). The HSV-1 gB conformation observed in the solved crystals (25) suggested to represent the postfusion form and a prefusion model of gB has not yet been characterized. Therefore, X-ray crystallographic studies of MAb 2c or its $F(ab')_2$ in complex with gB might provide insights into the native conformation of gB and a better understanding about transmission of the fusogenic signal.

Severe and even life-threatening HSV infections can occur in maternally infected newborns, in patients with recurrent ocular infections, or in severely immunocompromised patients. To investigate whether systemic application of our anti-gB antibody also confers protection in a highly immunodeficient *in vivo* setting, we employed a NOD/SCID mouse model. We used intravaginal HSV-1 inoculation as an established route of ganglionic infection, with axonal spread of the virus causing hind limb paralysis and fatal herpetic encephalitis in immunocompetent as well as in T-cell-depleted mice (17, 18). Here we demonstrate that MAb 2c not only fully protects NOD/SCID in the acute phase of primary HSV-1 infection but also is effective in completely preventing neurological disease and death even after peripheral virus spread has commenced. The HSV cell-to-cell spread is a very efficient way for virus to transfer across neuronal synapses and tight junctions as well as to circumvent immunological barriers of the adaptive immune system. MAb 2c both decreases virus expression of infected vaginal tissues and inhibits axonal spread of HSV. Other reports showed that administration of anti-HSV IgGs after viral challenge can reduce the quantity of acute ganglionic infections in animals (17, 43). Consistently, intraperitoneally administered recombinant human anti-gD IgG in mice with corneal HSV-1 infection was shown to localize to HSV-infected nerve fibers and sensory neurons (61). Furthermore, passive immunization of immunocompetent animals with MAbs specific for HSV gD, gC, or gB administered postexposure at appropriate times demonstrated protection against HSV-induced neurological disease (14, 17). However, it has also been concluded from several animal studies that humoral immunity alone is ineffective in the control of HSV infections. Consistent with this view, administration of anti-HSV-1 hyperimmune serum has been reported to be insufficient for protecting immunosuppressed or immunodeficient mice (48, 49, 52, 53, 58). Another study, in an HSV-1-induced stromal keratitis mouse model, showed that an anti-gD MAb prevented death of mice depleted of either $CD4^+$ or $CD8^+$ T cells but failed to prevent death when mice were depleted of both T-cell subsets simultaneously (66). On the other hand, intraperitoneal application of a human anti-gD MAb to athymic nude mice 24 h after intracutaneous HSV-1 infection was able to prevent death in 11% of the animals (60). Although the role of antibodies in resolving viral diseases is controversial, our *in vivo* data obtained in a severely immunocompromised setting clearly show that a monoclonal antibody can mediate full protection even after HSV reaches the peripheral nervous system. Therefore, these results encourage further development of monoclonal antibodies with properties comparable to those of MAb 2c for therapy of severe HSV diseases.

To our knowledge, we here demonstrate for the first time the protective efficacy of a systemically applied anti-gB cross-linking MAb that prevents neuronal HSV-1 spread completely independently from cellular effector mechanisms and complement.

## ACKNOWLEDGMENTS

This work was supported in part by Deutsche José Carreras Leukämie Foundation grant DJCLS R06/14 (J.K., A.M.E.-H., and M.R.), the Deutsche Forschungsgemeinschaft (GK-1045), and a research fellowship from the Jürgen Manchot Foundation (A.K.).

Recombinant gB(730)t was generously donated by Roselyn J. Eisenberg and Gary H. Cohen (University of Pennsylvania, Philadelphia). Leonore Pereira (University of California, San Francisco) kindly provided plasmids coding for gB deletion mutants. We thank Evelyn Exner for excellent technical assistance, Simone Schimmer, Kirsten Dietze, and Maike Nowak for assistance with the mouse models, and Claudia Dumitru and Bernd Giebel for help with the microscopic analysis.

## REFERENCES

1. **Arndt, M. A., et al.** 2003. Generation of a highly stable, internalizing anti-CD22 single-chain Fv fragment for targeting non-Hodgkin's lymphoma. Int. J. Cancer **107:**822–829.
2. **Ashkar, A. A., and K. L. Rosenthal.** 2003. Interleukin-15 and natural killer and NKT cells play a critical role in innate protection against genital herpes simplex virus type 2 infection. J. Virol. **77:**10168–10171.
3. **Atanasiu, D., et al.** 2007. Bimolecular complementation reveals that glycoproteins gB and gH/gL of herpes simplex virus interact with each other during cell fusion. Proc. Natl. Acad. Sci. U. S. A. **104:**18718–18723.
4. **Bender, F. C., et al.** 2007. Antigenic and mutational analyses of herpes simplex virus glycoprotein B reveal four functional regions. J. Virol. **81:**3827–3841.
5. **Bender, F. C., J. C. Whitbeck, H. Lou, G. H. Cohen, and R. J. Eisenberg.** 2005. Herpes simplex virus glycoprotein B binds to cell surfaces independently of heparan sulfate and blocks virus entry. J. Virol. **79:**11588–11597.
6. **Bizebard, T., et al.** 1995. Structure of influenza virus haemagglutinin complexed with a neutralizing antibody. Nature **376:**92–94.
7. **Blomberg, N., E. Baraldi, M. Nilges, and M. Saraste.** 1999. The PH superfold: a structural scaffold for multiple functions. Trends Biochem. Sci. **24:**441–445.
8. **Brown, Z. A., et al.** 1991. Neonatal herpes simplex virus infection in relation to asymptomatic maternal infection at the time of labor. N. Engl. J. Med. **324:**1247–1252.
9. **Burbelo, P. D., et al.** 2009. Serological diagnosis of human herpes simplex virus type 1 and 2 infections by luciferase immunoprecipitation system assay. Clin. Vaccine Immunol. **16:**366–371.
10. **Carter, C., S. Savic, J. Cole, and P. Wood.** 2007. Natural killer cell receptor expression in patients with severe and recurrent herpes simplex virus-1 (HSV-1) infections. Cell. Immunol. **246:**65–74.
11. **Co, M. S., M. Deschamps, R. J. Whitley, and C. Queen.** 1991. Humanized antibodies for antiviral therapy. Proc. Natl. Acad. Sci. U. S. A. **88:**2869–2873.
12. **Cook, M. L., and J. G. Stevens.** 1973. Pathogenesis of herpetic neuritis and ganglionitis in mice: evidence for intra-axonal transport of infection. Infect. Immun. **7:**272–288.
13. **Cunningham, A. L., R. R. Turner, A. C. Miller, M. F. Para, and T. C. Merigan.** 1985. Evolution of recurrent herpes simplex lesions. An immunohistologic study. J. Clin. Invest. **75:**226–233.
14. **Dix, R. D., L. Pereira, and J. R. Baringer.** 1981. Use of monoclonal antibody directed against herpes simplex virus glycoproteins to protect mice against acute virus-induced neurological disease. Infect. Immun. **34:**192–199.
15. **Donaghy, H., et al.** 2009. Role for plasmacytoid dendritic cells in the immune control of recurrent human herpes simplex virus infection. J. Virol. **83:**1952–1961.

16. **Drew, P. D., et al.** 2001. Multimeric humanized varicella-zoster virus antibody fragments to gH neutralize virus while monomeric fragments do not. J. Gen. Virol. **82:**1959–1963.
17. **Eis-Hubinger, A. M., K. Mohr, and K. E. Schneweis.** 1991. Different mechanisms of protection by monoclonal and polyclonal antibodies during the course of herpes simplex virus infection. Intervirology **32:**351–360.
18. **Eis-Hubinger, A. M., D. S. Schmidt, and K. E. Schneweis.** 1993. Anti-glycoprotein B monoclonal antibody protects T cell-depleted mice against herpes simplex virus infection by inhibition of virus replication at the inoculated mucous membranes. J. Gen. Virol. **74:**379–385.
19. **Fleury, D., et al.** 1999. A complex of influenza hemagglutinin with a neutralizing antibody that binds outside the virus receptor binding site. Nat. Struct. Biol. **6:**530–534.
20. **Fleury, D., S. A. Wharton, J. J. Skehel, M. Knossow, and T. Bizebard.** 1998. Antigen distortion allows influenza virus to escape neutralization. Nat. Struct. Biol. **5:**119–123.
21. **Frank, R., and H. Overwin.** 1996. SPOT synthesis. Epitope analysis with arrays of synthetic peptides prepared on cellulose membranes. Methods Mol. Biol. **66:**149–169.
22. **Grubor-Bauk, B., A. Simmons, G. Mayrhofer, and P. G. Speck.** 2003. Impaired clearance of herpes simplex virus type 1 from mice lacking CD1d or NKT cells expressing the semivariant V alpha 14-J alpha 281 TCR. J. Immunol. **170:**1430–1434.
23. **Hannah, B. P., et al.** 2009. Herpes simplex virus glycoprotein B associates with target membranes via its fusion loops. J. Virol. **83:**6825–6836.
24. **Hannah, B. P., E. E. Heldwein, F. C. Bender, G. H. Cohen, and R. J. Eisenberg.** 2007. Mutational evidence of internal fusion loops in herpes simplex virus glycoprotein B. J. Virol. **81:**4858–4865.
25. **Heldwein, E. E., et al.** 2006. Crystal structure of glycoprotein B from herpes simplex virus 1. Science **313:**217–220.
26. **Highlander, S. L., W. H. Cai, S. Person, M. Levine, and J. C. Glorioso.** 1988. Monoclonal antibodies define a domain on herpes simplex virus glycoprotein B involved in virus penetration. J. Virol. **62:**1881–1888.
27. **Kaufman, E. N., and R. K. Jain.** 1992. Effect of bivalent interaction upon apparent antibody affinity: experimental confirmation of theory using fluorescence photobleaching and implications for antibody binding assays. Cancer Res. **52:**4157–4167.
28. **Kipriyanov, S. M., O. A. Kupriyanova, M. Little, and G. Moldenhauer.** 1996. Rapid detection of recombinant antibody fragments directed against cell-surface antigens by flow cytometry. J. Immunol. Methods **196:**51–62.
29. **Koelle, D. M., et al.** 1998. Clearance of HSV-2 from recurrent genital lesions correlates with infiltration of HSV-specific cytotoxic T lymphocytes. J. Clin. Invest. **101:**1500–1508.
30. **Kohl, S.** 1991. Role of antibody-dependent cellular cytotoxicity in defense against herpes simplex virus infections. Rev. Infect. Dis. **13:**108–114.
31. **Kohl, S., D. L. Cahall, D. L. Walters, and V. E. Schaffner.** 1979. Murine antibody-dependent cellular cytotoxicity to herpes simplex virus-infected target cells. J. Immunol. **123:**25–30.
32. **Kohl, S., N. C. Strynadka, R. S. Hodges, and L. Pereira.** 1990. Analysis of the role of antibody-dependent cellular cytotoxic antibody activity in murine neonatal herpes simplex virus infection with antibodies to synthetic peptides of glycoprotein D and monoclonal antibodies to glycoprotein B. J. Clin. Invest. **86:**273–278.
33. **Kohl, S., et al.** 1989. Neonatal antibody-dependent cellular cytotoxic antibody levels are associated with the clinical presentation of neonatal herpes simplex virus infection. J. Infect. Dis. **160:**770–776.
34. **Kousoulas, K. G., B. Huo, and L. Pereira.** 1988. Antibody-resistant mutations in cross-reactive and type-specific epitopes of herpes simplex virus 1 glycoprotein B map in separate domains. Virology **166:**423–431.
35. **Kramer, A., and J. Schneider-Mergener.** 1998. Synthesis and screening of peptide libraries on continuous cellulose membrane supports. Methods Mol. Biol. **87:**25–39.
36. **Krummenacher, C., et al.** 2005. Structure of unliganded HSV gD reveals a mechanism for receptor-mediated activation of virus entry. EMBO J. **24:**4144–4153.
37. **Kuhn, J. E., G. Dunkler, K. Munk, and R. W. Braun.** 1987. Analysis of the IgM and IgG antibody response against herpes simplex virus type 1 (HSV-1) structural and nonstructural proteins. J. Med. Virol. **23:**135–150.
38. **Kwant-Mitchell, A., A. A. Ashkar, and K. L. Rosenthal.** 2009. Mucosal innate and adaptive immune responses against herpes simplex virus type 2 in a humanized mouse model. J. Virol. **83:**10664–10676.
39. **Lemmon, M. A., and K. M. Ferguson.** 2000. Signal-dependent membrane targeting by pleckstrin homology (PH) domains. Biochem. J. **350:**1–18.
40. **Li, W., T. J. Minova-Foster, D. D. Norton, and M. I. Muggeridge.** 2006. Identification of functional domains in herpes simplex virus 2 glycoprotein B. J. Virol. **80:**3792–3800.
41. **Lin, E., and P. G. Spear.** 2007. Random linker-insertion mutagenesis to identify functional domains of herpes simplex virus type 1 glycoprotein B. Proc. Natl. Acad. Sci. U. S. A. **104:**13140–13145.
42. **Lingen, M., F. Hengerer, and D. Falke.** 1997. Mixed vaginal infections of Balb/c mice with low virulent herpes simplex type 1 strains result in restoration of virulence properties: vaginitis/vulvitis and neuroinvasiveness. Med. Microbiol. Immunol. **185:**217–222.
43. **McKendall, R. R., T. Klassen, and J. R. Baringer.** 1979. Host defenses in herpes simplex infections of the nervous system: effect of antibody on disease and viral spread. Infect. Immun. **23:**305–311.
44. **Mester, J. C., J. C. Glorioso, and B. T. Rouse.** 1991. Protection against zosteriform spread of herpes simplex virus by monoclonal antibodies. J. Infect. Dis. **163:**263–269.
45. **Mikloska, Z., A. M. Kesson, M. E. Penfold, and A. L. Cunningham.** 1996. Herpes simplex virus protein targets for CD4 and CD8 lymphocyte cytotoxicity in cultured epidermal keratinocytes treated with interferon-gamma. J. Infect. Dis. **173:**7–17.
46. **Milligan, G. N., and D. I. Bernstein.** 1997. Interferon-gamma enhances resolution of herpes simplex virus type 2 infection of the murine genital tract. Virology **229:**259–268.
47. **Milligan, G. N., D. I. Bernstein, and N. Bourne.** 1998. T lymphocytes are required for protection of the vaginal mucosae and sensory ganglia of immune mice against reinfection with herpes simplex virus type 2. J. Immunol. **160:**6093–6100.
48. **Minagawa, H., S. Sakuma, S. Mohri, R. Mori, and T. Watanabe.** 1988. Herpes simplex virus type 1 infection in mice with severe combined immunodeficiency (SCID). Arch. Virol. **103:**73–82.
49. **Nagafuchi, S., H. Oda, R. Mori, and T. Taniguchi.** 1979. Mechanism of acquired resistance to herpes simplex virus infection as studied in nude mice. J. Gen. Virol. **44:**715–723.
50. **Navarro, D., P. Paz, and L. Pereira.** 1992. Domains of herpes simplex virus I glycoprotein B that function in virus penetration, cell-to-cell spread, and cell fusion. Virology **186:**99–112.
51. **Nielsen, U. B., G. P. Adams, L. M. Weiner, and J. D. Marks.** 2000. Targeting of bivalent anti-ErbB2 diabody antibody fragments to tumor cells is independent of the intrinsic antibody affinity. Cancer Res. **60:**6434–6440.
52. **Oakes, J. E.** 1975. Invasion of the central nervous system by herpes simplex virus type 1 after subcutaneous inoculation of immunosuppressed mice. J. Infect. Dis. **131:**51–57.
53. **Oakes, J. E.** 1975. Role for cell-mediated immunity in the resistance of mice to subcutaneous herpes simplex virus infection. Infect. Immun. **12:**166–172.
54. **Pereira, L., M. Ali, K. Kousoulas, B. Huo, and T. Banks.** 1989. Domain structure of herpes simplex virus 1 glycoprotein B: neutralizing epitopes map in regions of continuous and discontinuous residues. Virology **172:**11–24.
55. **Pereira, L., T. Klassen, and J. R. Baringer.** 1980. Type-common and type-specific monoclonal antibody to herpes simplex virus type 1. Infect. Immun. **29:**724–732.
56. **Posner, M. R., et al.** 1991. An IgG human monoclonal antibody that reacts with HIV-1/GP120, inhibits virus binding to cells, and neutralizes infection. J. Immunol. **146:**4325–4332.
57. **Qadri, I., C. Gimeno, D. Navarro, and L. Pereira.** 1991. Mutations in conformation-dependent domains of herpes simplex virus 1 glycoprotein B affect the antigenic properties, dimerization, and transport of the molecule. Virology **180:**135–152.
58. **Rager-Zisman, B., and A. C. Allison.** 1976. Mechanism of immunologic resistance to herpes simplex virus 1 (HSV-1) infection. J. Immunol. **116:**35–40.
59. **Reed, J. L., and H. Muench.** 1938. A simple method of estimating fifty percent endpoints. Am. J. Hyg. (London) **27:**493–497.
60. **Sanna, P. P., et al.** 1996. Protection of nude mice by passive immunization with a type-common human recombinant monoclonal antibody against HSV. Virology **215:**101–106.
61. **Sanna, P. P., T. J. Deerinck, and M. H. Ellisman.** 1999. Localization of a passively transferred human recombinant monoclonal antibody to herpes simplex virus glycoprotein D to infected nerve fibers and sensory neurons in vivo. J. Virol. **73:**8817–8823.
62. **Satoh, T., et al.** 2008. PILRalpha is a herpes simplex virus-1 entry coreceptor that associates with glycoprotein B. Cell **132:**935–944.
63. **Silverman, J. L., S. Sharma, T. M. Cairns, and E. E. Heldwein.** 2010. Fusion-deficient insertion mutants of herpes simplex virus type 1 glycoprotein B adopt the trimeric postfusion conformation. J. Virol. **84:**2001–2012.
64. **Smith, P. M., R. M. Wolcott, R. Chervenak, and S. R. Jennings.** 1994. Control of acute cutaneous herpes simplex virus infection: T cell-mediated viral clearance is dependent upon interferon-gamma (IFN-gamma). Virology **202:**76–88.
65. **Spear, P. G., and R. Longnecker.** 2003. Herpesvirus entry: an update. J. Virol. **77:**10179–10185.
66. **Staats, H. F., J. E. Oakes, and R. N. Lausch.** 1991. Anti-glycoprotein D monoclonal antibody protects against herpes simplex virus type 1-induced diseases in mice functionally depleted of selected T-cell subsets or asialo GM1+ cells. J. Virol. **65:**6008–6014.
67. **Subramanian, R. P., and R. J. Geraghty.** 2007. Herpes simplex virus type 1 mediates fusion through a hemifusion intermediate by sequential activity of glycoproteins D, H, L, and B. Proc. Natl. Acad. Sci. U. S. A. **104:**2903–2908.
68. **Yokota, T., D. E. Milenic, M. Whitlow, and J. Schlom.** 1992. Rapid tumor penetration of a single-chain Fv and comparison with other immunoglobulin forms. Cancer Res. **52:**3402–3408.